Flame-Made Pt/Ceria/Zirconia for Low-Temperature Oxygen Exchange

Wendelin J. Stark,[†] Jan-Dierk Grunwaldt,[†] Marek Maciejewski,[†] Sotiris E. Pratsinis,[‡] and Alfons Baiker*,[†]

Institute for Chemical and Bioengineering, Department of Chemistry and Applied Biosciences, ETH Hönggerberg, CH-8093 Zürich, Switzerland, and Particle Technology Laboratory, Department of Mechanical Engineering, ETH Zürich, CH-8092 Zürich, Switzerland

Received March 9, 2005. Revised Manuscript Received April 27, 2005

The preparation of platinum (0−2 wt %) supported on ceria/zirconia ($Ce_{0.5}Zr_{0.5}O_2$) by flame synthesis resulted in materials with good thermal stability and improved dynamic oxygen exchange capacity at low temperatures. Comparison to a conventionally prepared material (precipitation and incipient wetness impregnation) showed an increased specific surface area for the flame-made catalysts after sintering at 1100 °C for 6 h in air. For low Pt content (0.1−0.5 wt %), the onset in low-temperature oxygen exchange activity of flame-made materials was even improved after a first redox test run. Repeated test runs up to 1100 °C deactivated the reference material for oxygen exchange below 300 °C, while the flame-made materials showed improved activity down to around 150 °C. Fluorescence EXAFS revealed the presence of oxidized Pt on the pre-sintered materials and confirmed the role of reduced Pt on the hydrogen activation prior to oxygen exchange. It further uncovered pronounced differences in Pt reducibility depending on the Pt loading.

Introduction

Exhaust gas catalysis has made significant progress over the last 2 decades and novel catalytic materials have strongly reduced emissions from automotive combustion sources.[1−3] Today, platinum group noble metals are mainly consumed for catalysis. One-third of platinum, half of palladium, and most rhodium are used for exhaust gas cleaning.[4] Consequently, their prices are high and now make up for a good part of costs in the catalytic process. The development toward even more efficient exhaust gas catalysis is largely hindered by the limited availability of these metals and their prices. Different attempts have been made to reduce the required amounts of noble metals in catalysis, and recycling today somewhat eases the shortage of platinum metals.[5] Research on single Au and Pt site catalysts has recently revealed exceptionally high rates for the water−gas shift reaction at low noble metal loadings.[6] Since such high dispersions may be favored by rapid cooling, flame synthesis of noble metal based materials was suggested to result in catalysts with lower platinum consumption. Flame synthesis has recently been shown to give access to a series of catalysts.[7−15] It has become clear that the relatively open morphology of gas-phase made materials could reduce mass transfer limitations and contribute to more efficient noble metal catalysis.[16] Strobel et al. found a more than 2-fold increase in hydrogenation rate when using a flame-made catalyst instead of a commercially available precipitated material, despite similar specific surface area.[15] The preparation of ceria/zirconia by flame synthesis yielded materials with high thermal stability, but it was not accompanied by an improved dynamic oxygen exchange capacity.[12,17] The addition of alumina or silica did increase the oxygen exchange capacity[18] while good thermal stability was maintained, motivating us for the present study.

Here, we report that the high-temperature flame process can be adapted to the synthesis of platinum on ceria/zirconia in a single step. Comparison of the materials to conventionally prepared ones revealed improved low-temperature oxygen exchange activity and thermal stability. In situ fluorescence EXAFS was applied for determining the reduction behavior of the materials, even at very low noble metal

* Corresponding author. Phone: +41 1632 3153. Fax: +41 1632 11 63. E-mail: alfons.baiker@chem.ethz.ch.
[†] ETH Hönggerberg.
[‡] ETH Zürich.

(1) Trovarelli, A. *Catal. Sci. Ser.* **2002**, *2*, 508.
(2) Gandhi, H. S.; Graham, G. W.; McCabe, R. W. *J. Catal.* **2003**, *216*, 433−442.
(3) Di Monte, R.; Kaspar, J. *J. Mater. Chem.* **2005**, *15*, 633−648.
(4) Cowley, A. *Platinum 2004*; Johnson Matthey: London, 1999.
(5) Kim, C. H.; Woo, S. I.; Jeon, S. H. *Ind. Eng. Chem. Res.* **2000**, *39*, 1185.
(6) Fu, Q.; Saltsburg, H.; Flytzani-Stephanopoulos, M. *Science* **2003**, *301*, 935.
(7) Johannessen, T.; Koutsopoulos, S. *J. Catal.* **2002**, *205*, 404−408.
(8) Backman, U.; Tapper, U.; Jokiniemi, J. K. *Synth. Met.* **2004**, *142*, 169−176.
(9) Hinklin, T.; Toury, B.; Gervais, C.; Babonneau, F.; Gislason, J. J.; Morton, R. W.; Laine, R. M. *Chem. Mater.* **2004**, *16*, 21−30.
(10) Stark, W. J.; Wegner, K.; Pratsinis, S. E.; Baiker, A. *J. Catal.* **2001**, *197*, 182−191.
(11) Stark, W. J.; Pratsinis, S. E.; Baiker, A. *J. Catal.* **2001**, *203*, 516−524.
(12) Stark, W. J.; Pratsinis, S. E. *Powder Technol.* **2002**, *126*, 103−108.
(13) Stark, W. J.; Maciejewski, M.; Madler, L.; Pratsinis, S. E.; Baiker, A. *J. Catal.* **2003**, *220*, 35−43.
(14) Strobel, R.; Stark, W. J.; Madler, L.; Pratsinis, S. E.; Baiker, A. *J. Catal.* **2003**, *213*, 296−304.
(15) Strobel, R.; Krumeich, F.; Stark, W. J.; Pratsinis, S. E.; Baiker, A. *J. Catal.* **2004**, *222*, 307−314.
(16) Rolison, D. R. *Science* **2003**, *299*, 1698.
(17) Stark, W. J.; Madler, L.; Maciejewski, M.; Pratsinis, S. E.; Baiker, A. *Chem. Commun.* **2003**, 588−589.
(18) Schulz, H.; Stark, W. J.; Maciejewski, M.; Pratsinis, S. E.; Baiker, A. *J. Mater. Chem.* **2003**, *13* (12), 2979−2984.

10.1021/cm050538+ CCC: $30.25
Published on Web 05/25/2005

loadings (0.1 wt % Pt) and corroborated structural differences in Pt/ceria/zirconia dependent on their preparation.

Experimental Section

Powder Preparation. Pt/ceria/zirconia nanoparticles were prepared by flame spray pyrolysis[17,19] using corresponding precursor mixtures of cerium 2-ethylhexanoate (Strem, 99%), zirconium 2-ethyl hexanoate (Strem, 99%), and platinum acetylacetonate (Strem, 98%) dissolved in 2-ethylhexanoic acid (purum, ≥99%, Fluka)/xylene (96%, Riedel deHaen) at a final concentration of 0.2 M cerium and zirconium each. The liquid mixtures were fed through a capillary (diameter 0.4 mm) into a methane/oxygen flame at 5 mL/min. Oxygen (5 L/min, 99.8%, Pan Gas, constant pressure drop at the capillary tip 1.5 bar) was used to disperse the liquid leaving the capillary. A stable combustion was achieved by applying a sheath gas (oxygen, 3.7 L/min, 99.8% Pan Gas) through a concentric sintered-metal ring. Calibrated mass flow controllers (Bronkhorst) were used to monitor all gas flows. The as-formed particles were collected on a glass-fiber filter (Whatmann GF/A, 25.7 cm in diameter) placed on a cylinder mounted above the flame, by the aid of a vacuum pump (Vaccubrand).

A reference material was prepared by coprecipitation of cerium and zirconyl nitrate solutions (0.2 M in water) by concentrated ammonium hydroxide solution (25 wt %), aging, and calcination according to Bonneau et al.[32] The Pt was then deposited onto the ceria/zirconia by impregnation according to Silvestre-Alberto et al.[33] using chlorine-free platinum acetylacetonate in ethanol.

X-ray diffraction was conducted on a Siemens powder X-ray diffractometer using Ni-filtered Cu Kα radiation in step mode with a step size of 0.01° and 2 s. Transmission electron microscopy images were recorded on a CM30 ST (Philips, LaB6 cathode, operated at 300 kV, point resolution ∼ 4 Å). Particles were deposited onto a carbon foil supported by a copper grid. The specific surface area of the powders was measured on a Tristar (Micromeritics Instruments) by nitrogen adsorption at 77 K using the Brunauer−Emmett−Teller (BET) method. All samples were outgassed at 150 °C for 1 h. For examination of the hydrogen uptake at 298 K, an Autochem (Micromeritics) was used with 1 mL pulses of 4.8% hydrogen in argon. Samples were reduced under flowing hydrogen at 350 °C prior to measurements. Elemental analysis (Pt content) was performed by laser ablation inductively coupled plasma mass spectroscopy.[20]

In Situ Fluorescence EXAFS Measurements. In situ fluorescence EXAFS experiments were performed at DESY (DORIS III ring operating at 4.4 GeV and an injection current of 140 mA) using a Si(111) double crystal for monochromatization. By detuning the crystals to 70% of the maximum intensity, higher harmonics were effectively eliminated. Measurements were carried out in a continuous-flow reactor cell allowing simultaneous gas analysis and structural studies.[21] Due to the strongly absorbing matrix (CeO_2-ZrO_2), transmission EXAFS experiments did not lead to reasonable signal-to-noise ratio at the Pt L_3-edge. We therefore applied in situ XANES/EXAFS in the fluorescence mode. A seven-element Si(Li) detector (Gresham) was applied to measure the fluorescence X-rays of Pt as function of the excitation energy. For this purpose, the catalyst sample was loaded in a capillary and fixed at 45° to the beam, with the fluorescence detector being placed 90° to the beam[21,22] as proposed by Kappen et al.[23] An external gas supply provided different, premixed gases through the capillary cell and the samples were analyzed with a mass spectrometer (Balzers, Thermostar). Enclosing the sample in an X-ray-transparent heat shield (Kapton) ensured temperature homogeneity around the irradiated sample. The reduction was performed in situ by using 5% H_2/He and a continuous heating ramp of 5 °C/min.

The fluorescence signals from the seven detector channels were amplified, and shaped detector signals were fed to analog-to-digital converters (Canberra 8715 ADCs) and further transferred to multichannel analyzers (MCAs). To determine the fluorescence stemming from Pt, software SCAs (single channel analyzers) were set around the Pt L_α-fluorescence line. At each monochromator energy, the integral values of the seven software SCAs were stored as well as the MCA spectra. Typically, EXAFS scans were taken between 11 430 and 12 400 eV (60 min/scan) and faster XAS scans during dynamic changes between 11 540 and 11 650 eV (1−3 min/scan). The raw data were energy-calibrated with measurement of a Pt foil, background-corrected, normalized, and fitted using the WINXAS 3.0 package.[24] During reduction and oxidation of the Pt constituent, the extent of reduction or oxidation was calculated by a linear combination of the starting and end spectra or appropriate reference data.

Dynamic Oxygen Exchange Capacity (DOEC) Analysis. Prior to analysis, samples were pretreated in air at 700 °C for 16 h with a heating/cooling rate of 5 °C/min. The dynamic oxidation and reduction behavior was studied by isothermal (700 °C) and nonisothermal thermoanalytical experiments on a thermoanalyzer (Netzsch STA 409) equipped with a gas injector (dual-external sample injector, Valco Instruments). It enabled the injection of specified amounts of probe gas (H_2, O_2) into the inert carrier gas stream.[25] Gases evolved during the reaction were monitored on-line with a quadrupole mass spectrometer (Balzers QMG 420) connected to the thermoanalyzer by a heated capillary. Changes in sample mass resulting from oxygen removal due to pulses of hydrogen (2 mL) were taken as a measure of the dynamic oxygen exchange capacity (OEC). In nonisothermal experiments, samples were reduced by 4 mL pulses of H_2 in order to supply excess of reducing agent even at temperatures as high as 1000 °C. After reduction, the samples were reoxidized by pulses of oxygen (1 mL in isothermal, 2 mL for nonisothermal runs). The overall sample mass was unaffected by a full reduction/oxidation step that corroborated the full reversibility of the redox process. The oxygen exchange capacity was expressed in micrograms of O_2 removed during reduction of a 50.00-mg sample.

Results and Discussion

Structural Characterization. Flame synthesis of the ternary system Pt/ceria/zirconia with 0−2 wt % Pt on

(19) Mädler, L.; Stark, W. J.; Pratsinis, S. E. *J. Mater. Res.* **2002**, *17*, 1356.
(20) Gunther, D.; Frischknecht, R.; Heinrich, C. A.; Kahlert, H. J. *J. Anal. At. Spectrom.* **1997**, *12*, 939−944.
(21) Grunwaldt, J. D.; Caravati, M.; Hannemann, S.; Baiker, A. *Phys. Chem. Chem. Phys.* **2004**, *6*, 3037.
(22) Grunwaldt, J. D.; Hannemann, S.; Göttlicher, S.; Mangold, M.; Denecke, A.; Baiker, A. *Phys. Scr.* **2005**, *T115*, 769−771.
(23) Kappen, P.; Grunwaldt, J. D.; Hammershoi, B. S.; Tröger, L.; Materlik, G.; Clausen, B. S. *J. Catal.* **2001**, *198*, 56.
(24) Ressler, T. *J. Synchr. Radiat.* **1998**, *5*, 118.
(25) Maciejewski, M.; Müller, C. A.; Tschan, R.; Emmerich, W. D.; Baiker, A. *Thermochim. Acta* **1997**, *295*, 167.
(26) Sinfelt, J. H.; Carter J. L.; Yates, D. J. C. *J. Catal.* **1972**, *24*, 283−296.
(27) Gatica, J. M.; Baker, R. T.; Fornasiero, P.; Bernal, S.; Kaspar, J. *J. Phys. Chem. B* **2001**, *105*, 1191−1199.
(28) Fornasiero, P.; Kaspar, J.; Montini, T.; Graziani, M.; Dal Santo, V.; Psaro, R.; Recchia, S. *J. Mol. Catal. A* **2003**, *204*, 683−691.
(29) Hickey, N.; Fornasiero, P.; Kaspar, J.; Gatica, J. M.; Bernal, S. *J. Catal.* **2001**, *200*, 181−193.
(30) Hori, C. E.; Brenner, A.; Ng, K. Y. S.; Rahmoeller, K. M.; Belton, D. *Catal. Today* **1999**, *50*, 299−308.
(31) Suda, A.; Yamamura, K.; Sobukawa, H.; Ukyo, Y.; Tanabe, T.; Nagai Y.; Dong, F.; Sugiura, M. *J. Ceram. Soc. Jpn.* **2004**, *112*, 623−627.
(32) Bonneau L.; Chopin, T.; Vilmin, G.; Touret, O. US Patent 5,908,800.
(33) Silvestre-Alberto, J.; Rodriguez-Reinoso, F.; Sepulveda-Escribano, A. *J. Catal.* **2002**, *210*, 127−136.

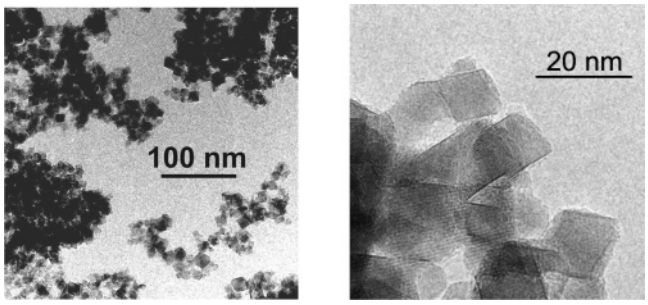

Figure 1. Electron microscopy images of 1 wt % Pt on $Ce_{0.5}Zr_{0.5}O_2$ as prepared by flame synthesis (left) and after calcination at 700 °C, for 16 h in air showing 10−25 nm highly crystalline mixed-oxide nanoparticles.

Table 1. Structural Properties of Pt/Ceria/Zirconia

	% Pt content		BET area/m^2 g^{-1}		H_2 chemisorption[d]/
sample	nominal	measured[a]	700 °C[b]	1100 °C[c]	H/Pt
0 Pt	0	0.00	84	4.5	−
0.1 Pt	0.1	−	78	3.5	−
0.5 Pt	0.5	0.51	79	4.3	1.7
1 Pt	1	0.98	84	4.0	1.3
2 Pt	2	2.10	98	−	0.8
ref	0.5	−	30	1.0	−

[a] Measured by laser-ablation ICP-MS; error ±5%. [b] After sintering at 700 °C, for 16 h, in air; after preparation, 105 m^2/g; error ±3%. [c] After sintering at 1100 °C, for 6 h, in air; error ±10%. [d] Measured at 298 K; error ±10%.

$Ce_{0.5}Zr_{0.5}O_2$ resulted in sharp-edged, highly crystalline nanoparticles of 10−25 nm size grouped in small agglomerates as revealed by TEM (Figure 1). The structural properties of these materials are summarized in Table 1. After calcination at 700 °C for 16 h, the specific surface area reached around 80−100 m^2/g compared to 30 m^2/g for the conventionally prepared reference material. Sintering at 1100 °C for 6 h in air still afforded a material with about 4 m^2/g. Compared to a similarly treated conventionally prepared material with around 1 m^2/g, this corroborated the good thermal stability of flame-made ceria/zirconia.[17] In agreement with studies on Pt/alumina, the noble metal showed little influence on the sintering of the support.[14] Platinum was regularly distributed and no Pt agglomerates could be detected by energy-dispersive X-ray analysis in transmission electron microscopy. Earlier synthesis of Pt/alumina reported similarly high dispersion, corroborating the advantage of high-temperature gas-phase deposition of platinum.[14] The lack of Pt lumps correlates well with the hydrogen uptake measured by chemisorption.[26] The hydrogen chemisorption data indicate that the determination of Pt dispersion is obscured by hydrogen spillover[27] at least for samples with low Pt loading. Similar high values were obtained by Fornasiero et al. for samples with 1.5 wt % Pt[28] and by Hickey et al. for samples with 0.5 wt % Pt.[29] At low Pt loadings, the lack of Pt signals in X-ray diffraction pattern of calcined samples is attributed to the presence of PtO_x and the high dispersion of Pt metal on the support. Fluorescence EXAFS and reduction profiles further supported the presence of oxidized Pt and a high Pt dispersion.

Dynamic Oxygen Exchange Capacity. An important property for possible applications in car exhaust gas cleaning is the dynamic oxygen exchange capacity.[2,12,18,25] Consequently, materials were subjected to a series of reducing (hydrogen) or oxidizing (oxygen) pulses while the temperature increased (see Figure 2). Simultaneous monitoring of the sample mass (thermobalance) and gas composition (mass spectrometer) allowed determination of the amount of dynamically stored oxygen in the samples. Ceria/zirconia with increasing amounts of Pt (0−2 wt % Pt) were subjected to two subsequent test runs from room temperature up to 1100 °C. The results are summarized in Figures 3 and 4. At high temperature, i.e., above 700 °C, all flame-made materials behaved very similarly in terms of oxygen storage capacity. At lower temperature, however, striking differences were observed depending on Pt content (Figure 3) and the method of preparation (Figure 4). Note that the mass loss of a corresponding 50-mg sample of Pt-free $Ce_{0.5}Zr_{0.5}O_2$ due to the reduction of Ce(IV) to Ce(III) amounts to 1354 μg. For the sample containing 1% Pt, when all platinum is in the form of PtO_x, the additional mass loss due to the reduction

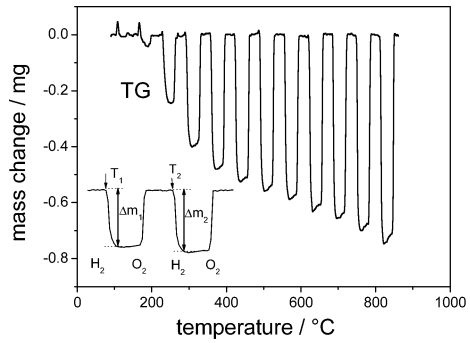

Figure 2. Measurement of total oxygen exchange capacity (OEC) showing fully reversible mass loss due to removed oxygen after a hydrogen pulse. Reoxidation by an oxygen pulse brought the sample back to the original mass. The OEC strongly increased with temperature. Insert: Determination of the mass loss for a given temperature.

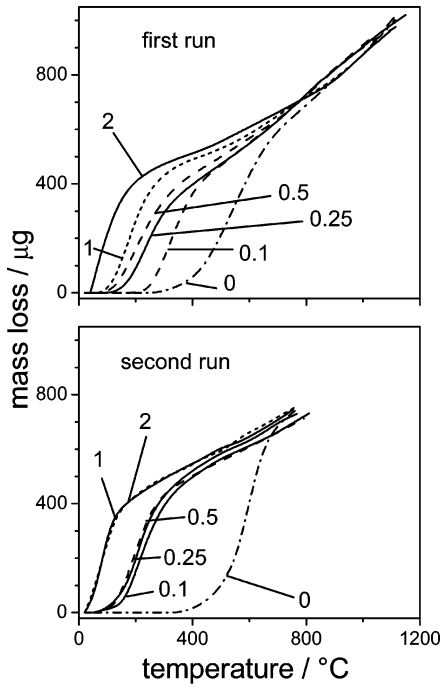

Figure 3. Oxygen exchange capacity of flame-made Pt/$Ce_{0.5}Zr_{0.5}O_2$ samples as measured by mass loss due to oxygen removal at different temperature (Figure 2). The Pt loading in weight percent is marked on the curves. Samples (50 mg) were measured in a first run (top) and then again in a second run (bottom) resulting in a strong increase in low-temperature activity.

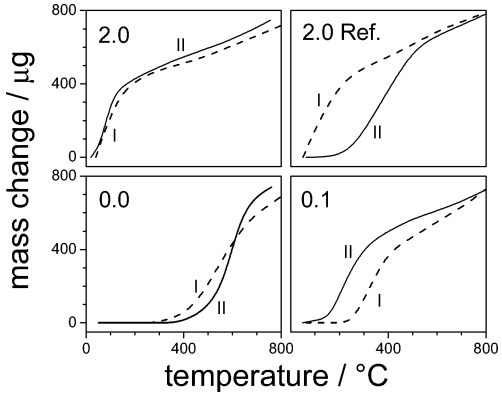

Figure 4. Comparison of the oxygen exchange capacity of 0, 0.1, and 2 wt % Pt/$Ce_{0.5}Zr_{0.5}O_2$ prepared by flame synthesis and conventionally prepared (according to the patent literature[32,33]) 2 wt % Pt/$Ce_{0.5}Zr_{0.5}O_2$. For testing the material stability, samples were subjected to catalytic test runs twice. First and second runs are marked as I and II, respectively. Sample mass, 50 mg.

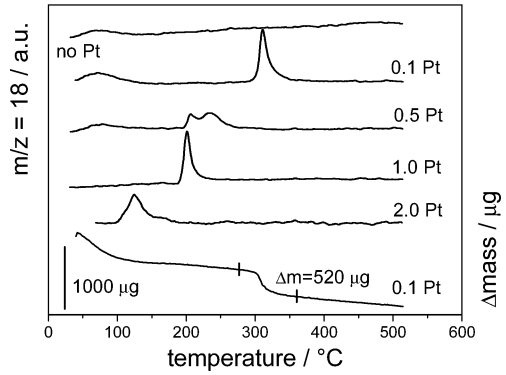

Figure 5. Evolution of water during reduction by 10 vol % H_2/Ar of different Pt loaded $Ce_{0.5}Zr_{0.5}O_2$ samples for increasing temperature monitored by TG combined with MS. The change of the mass (TG curve) of 0.1 wt % Pt/$Ce_{0.5}Zr_{0.5}O_2$ is given at the bottom. The stoichiometric mass loss due to the reduction of the amount of PtO_2 being equivalent to the Pt loading in the sample amounts to 7.0 μg, corroborating a strong reduction of the support.

of platinum oxide to metallic platinum amounts to 38 μg, i.e., ca 5% of the observed mass loss at 800 °C. For the sample containing 0.1% Pt, the mass loss due to the reduction of PtO_x amounts to ca. 0.5% of the total mass loss. The results presented in Figures 3 and 4 describe therefore basically the reduction of the support only and no information on the state of Pt is gained.

Influence of Platinum Loading. Measurement of different Pt/ceria/zirconia samples during the first run up to 1100 °C revealed a strong influence of the noble metal content. While pure ceria/zirconia started to exchange oxygen (reduction) above 400 °C, addition of 0.1 wt % platinum strongly activated the material and dynamic oxygen exchange already occurred around 200 °C (Figure 3). This is consistent with earlier investigations on precipitated ceria/zirconia supports by Hickey et al.[29] Further increasing the amount of Pt promoted the low-temperature activity. A Pt loading above 1 wt % did not lead to a much higher activity, and as a result of this, a sample with 2 wt % Pt was not much more active. The continuous increase of low-temperature activity at low Pt loading is consistent with earlier investigations.[29−31] In terms of loading or OEC onset, flame-made or precipitated materials behaved similarly during the first test run.

Thermal Stability. Earlier investigations on flame-made ceria/zirconia confirmed improved stability against sintering temperatures as high as 900 °C.[12,17] Interestingly, in the second run of oxygen exchange capacity measurements, increased low-temperature activity was found for samples with a low Pt content and the activity profiles appeared much different from those of the first run (Figure 3). Pt contents of 0.1−0.5 wt % resulted in almost the same degree of activity, and samples with 1 or 2 wt % Pt displayed the same oxygen exchange behavior.

Comparison to Reference Materials. The same pretreatment (16 h, 700 °C, air) as for flame-made samples was applied prior to measurements of precipitated Pt/ceria/zirconia. Figure 4 compares the dynamic oxygen exchange capacity of the reference material, pure flame-made ceria/zirconia, and flame-made samples containing 0.1 or 2 wt % Pt. The activity of the reference material during the first test run up to 1100 °C was similar to that of the flame-made sample. However, in the second run, strong deactivation led to a loss in low-temperature activity.

Reduction Behavior. The activation of the flame-made materials during the second run and the loss of low-temperature activity of the reference material were found to be related to the change of the nature of the Pt constituent. Temperature-programmed reduction of the samples with increasing Pt contents (Figure 5) showed a steady shift of the reduction peak to a temperature as low as 120 °C. Even though the correlation of static (TPR) and dynamic data (OEC) is sometimes critical,[34] the same trend is visible if only considering first run data (Figure 3). The mass loss detected for sample 0.1 wt % Pt (Figure 5, bottom) proves the reduction of the support, since reduction of Pt^{2+} alone would only account for about 1% of the observed mass loss. This strong change in reduction properties after a first run is also observed at higher Pt loading. The similar degree of oxygen loss or reduction in both samples 0.1 and 1 wt % Pt further corroborates that the ceria support is reduced itself with the aid of the noble metal.

Obviously, Pt plays an important role in the reduction of the CeO_2-ZrO_2 support and thus the dynamic oxygen storage capacity. Hence, it is desirable to identify the oxidation state and the structure of platinum during reduction and after reoxidation. X-ray photoelectron spectroscopy and X-ray absorption are well-suited tools, but the loading of 0.1 wt % Pt is too small for XPS measurements, and in situ studies are hardly amenable. Moreover, transmission EXAFS experiments fail due to the parasitic absorption of X-rays by both ceria and zirconia. An edge jump of $\mu d = 0.01$ at the Pt L_3-edge was expected for the 1 wt % Pt/CeO_2-ZrO_2 sample at an absorption length of 1.5 and it would be even smaller for the 0.1 wt % Pt-doped sample. Hence, we applied in situ XANES/EXAFS in the fluorescence mode during reduction of the sample. The analysis uncovered that platinum was in the oxidized state in the sintered samples before testing. The spectra in Figures 6 and 7 show the

(34) Hickey, N.; Fornasiero, P.; Di Monte, R.; Kaspar, J.; Graziani, M.; Dolcetti, G. *Catal. Lett.* **2001**, *72*, 45−50.

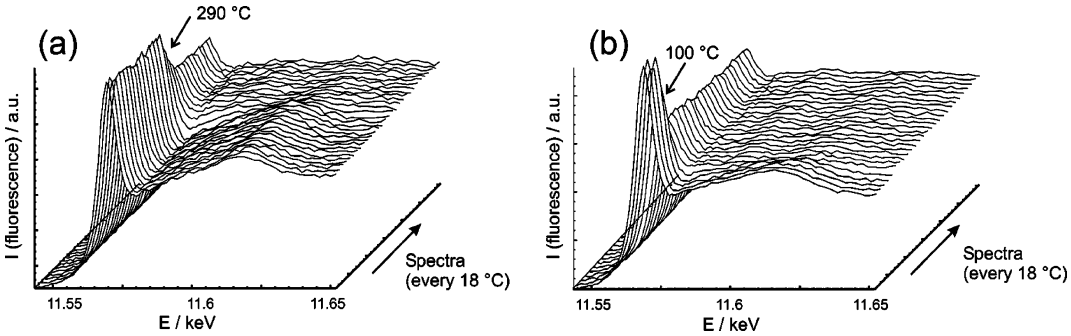

Figure 6. In situ reduction of 1 wt % $Pt/Ce_{0.5}Zr_{0.5}O_2$ monitored by fluorescence EXAFS at the Pt L_3-edge (5% H_2/He): (a) reduction behavior of the as-prepared sample and (b) reduction behavior of the reduced sample after reoxidation at 500 °C.

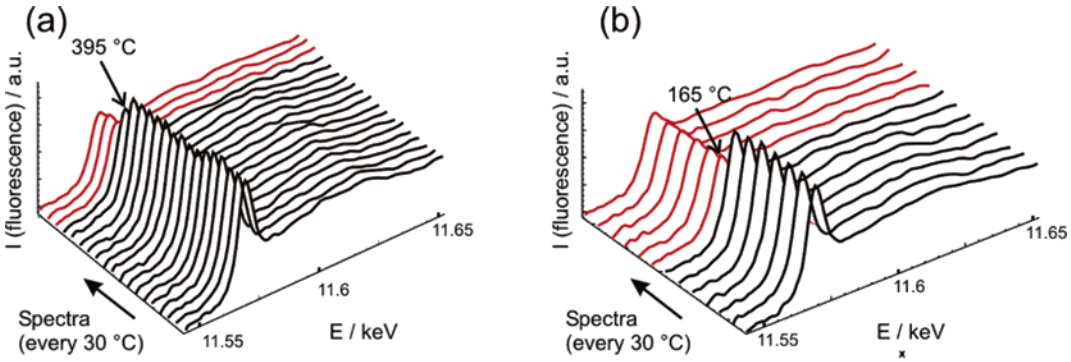

Figure 7. In situ reduction of 0.1 wt % $Pt/Ce_{0.5}Zr_{0.5}O_2$ monitored by fluorescence EXAFS at the Pt L_3-edge (5%H_2/He): (a) reduction behavior of the as-prepared sample and (b) reduction behavior of the reduced sample after reoxidation at 500 °C.

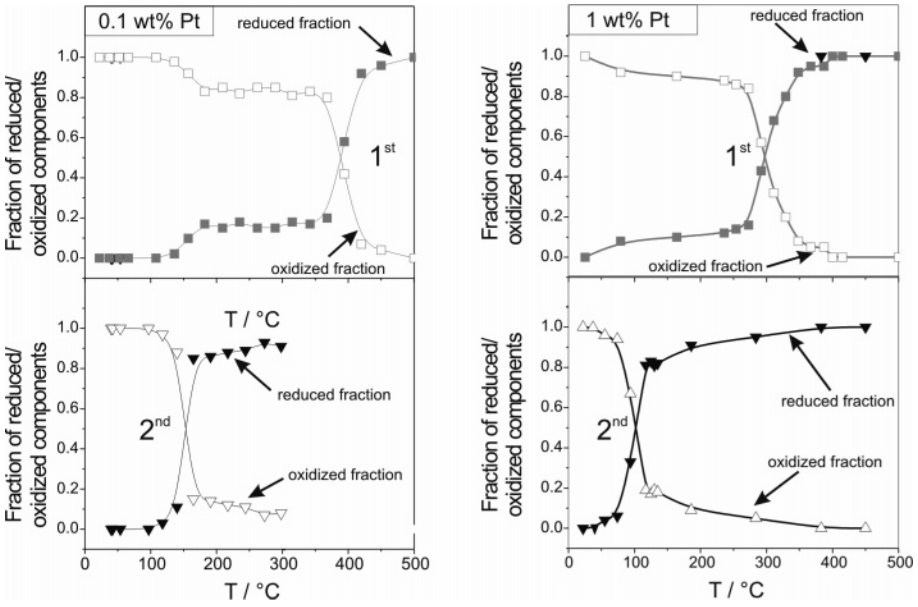

Figure 8. Comparison of the reduction behavior of Pt in 0.1 wt % $Pt/Ce_{0.5}Zr_{0.5}O_2$ and 1 wt % $Pt/Ce_{0.5}Zr_{0.5}O_2$ after the first (top) and the second (bottom) reduction in 5%H_2/He (2nd reduction after reoxidation at 500 °C in air), analyzed by linear combination analysis of the EXAFS spectra.

fluorescence data during in situ reduction of the catalysts. Platinum is reduced during the first run at 290 and 395 °C, respectively. The simultaneously recorded mass spectra uncovered that the reduction of the support also occurred at different temperature. This proves that reduction of the CeO_2-ZrO_2 matrix is facilitated in the presence of Pt^0. Another interesting fact is that platinum is much more difficult to reduce if it is present in small concentration, probably due to higher dispersion and stronger interaction with the support. The reduction is much easier if the platinum was once reduced (Figures 3, 6b, 7b). Figure 8 shows the quantitative data for the reduction of the noble metal, analyzed by linear combination of the XAS spectra (starting and end spectrum). During the first run, a 0.1 wt % Pt sample showed a maximal rate of reduction around 400 °C. This reduction temperature is shifted to 150 °C during a second run (after reoxidation in air at 500 °C). Correspondingly, the platinum constituent in the 1 wt % Pt/CeO_2-ZrO_2 sample is reduced around 300 °C during the first reduction and the reduction onset temperature is shifted to 100 °C during the second run. Obviously, platinum is finely dispersed on the support after preparation. The first reduction run in which

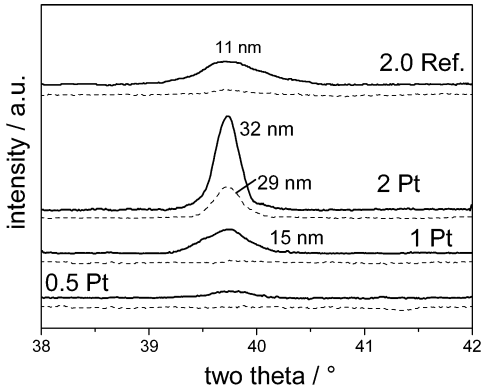

Figure 9. X-ray diffraction pattern of flame-made and reference materials after sintering at 700 °C, for 16 h in air (dashed) and after a test run up to 1100 °C (solid line). The pattern of the precipitated material indicates smaller Pt crystallites than the flame-made ones. Below 0.5 wt % Pt, no Pt reflections could be detected.

Scheme 1. Illustration of the Influence of the PtO_x Reduction Behavior on the Activation of Hydrogen[a]

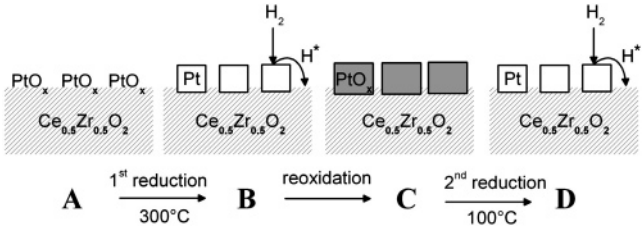

[a] The sintering of platinum particles after the first reduction (A → B) leads to lowering of the reduction temperature in the second reduction (C → D).

metallic Pt was exposed to hydrogen atmosphere at 500 °C led to a decrease in dispersion and, consequently, to a weaker support interaction of PtO_x particles formed during reoxidation. This resulted in lowering of the temperature of PtO_x reduction during the second run (see bottom plots in Figure 8) and in turn to a distinctly lower temperature of oxygen removal (see Figures 3 and 4) due to the presence of Pt^0 already at 100 °C. This behavior, illustrated in Scheme 1, underlines the important role of Pt^0 in the activation of hydrogen, which reduces the flame-made CeO_2-ZrO_2 sample by spillover at very low temperatures.[28,35]

Optimal Pt Loading. X-ray diffraction patterns of the same samples taken before (dashed) and after a test run up to 1100 °C are depicted in Figure 9. Flame-made materials at higher Pt loading show less prominent line broadening of the Pt reflections, indicating the presence of larger crystallites than in the reference material. At low loading, however, the XRD signals are too weak for detection. The appearance of larger crystallites indicates that Pt is relatively mobile at elevated temperature. While at low Pt loadings the Pt particles are well-dispersed and strongly stabilized by the ceria/zirconia matrix, above 1 wt % Pt saturation seems to occur and the additional Pt is accumulated in larger crystallites (Figure 9). Therefore, basically no differences in oxygen exchange behavior are observable for samples containing 1 or 2 wt % Pt after a second redox run (Figures 3 and 4). Hydrogen must be activated prior to reducing ceria within the support. In the case of pure ceria/zirconia, at least 500 °C is necessary to appreciably split hydrogen for reducing the ceria component. The addition of Pt results in low-temperature activity, since hydrogen is activated by Pt. At low Pt loadings (<0.5 wt % Pt), all Pt is contributing to the activation of hydrogen and a constant gain in activity results from increasing Pt contents from 0.1 to 1 wt % if only considering second runs, e.g., aged samples. Consequently, the 2 wt % Pt sample is not significantly more active than the 1 wt % Pt sample. These observations are in line with investigations by Suda et al. on ceria-zirconia with increasing Pt loading, where a similar saturation could be observed.[31]

Conclusions

The present results show that the preparation methods for Pt on ceria/zirconia can significantly influence the thermal stability and the oxygen exchange behavior. Flame-made Pt (0−2 wt %) on $Ce_{0.5}Zr_{0.5}O_2$ has been compared to a corresponding reference material (2 wt % Pt) derived by conventional wet chemical methods. Beyond physical characterization, samples were subjected to pulses of hydrogen and oxygen at temperatures up to 1100 °C to test their oxygen exchange behavior. While conventionally prepared and flame-made $Pt/Ce_{0.5}Zr_{0.5}O_2$ both exhibited low-temperature oxygen exchange capacity starting around 100 °C, the conventionally prepared material lost most of its low-temperature activity after a test run to 1100 °C. In contrast, the flame-made materials were not affected by such thermal treatment and improved their low-temperature activity. Fluorescence EXAFS proved to be well-suited for identifying structures at low concentrations, even in a highly absorbing matrix. The different reduction behavior of platinum at low concentration compared to that at higher concentration and its dependence on the history of the sample (prereduced or as-prepared, Scheme 1) demonstrates the importance of in situ characterization. Together with TPR, fluorescence EXAFS suggests an intrinsic difference in reducibility of the corresponding materials. Particularly at low Pt-loading, a prereduction of the Pt-doped ceria−zirconia materials was beneficial for the low-temperature DOE capacity. Pt L_3-XAS data taken in fluorescence mode proved that the reduction of the Pt constituent strongly depended on the history of the sample. The structural changes during the first and second reduction cycle are illustrated in Scheme 1. Due to sintering of Pt during the first reduction cycle, PtO_x obtained after reoxidation is more easily reduced during a second cycle. This leads to a higher DOE capacity at lower temperature because of hydrogen spillover from the Pt particle to the support. The present results may encourage further investigations on the use of flame-made materials for possible applications in high-temperature environments such as those existing in three-way catalysts for automotive exhaust treatment.

Acknowledgment. We thank the Hamburger Synchrotronstrahlungslabor (HASYLAB at DESY, Hamburg, Germany) for providing beamtime and J. Wienold and E. Welter for their kind help with setting up the Si(Li)-detector and for the intensive

(35) Hickey, N.; Fornasiero, P.; Kaspar, J.; Graziani, M.; Blanco, G.; Bernal, S. *Chem. Commun.* **2000**, 357−358.

discussion. Moreover, we thank S. Hannemann and M. Casapu for their help during the measurements at HASYLAB; N. Osterwalder, R. Strobel, and H. Schulz for sample preparation; and Dr. F. Krumeich for transmission electron microscopy. We thank Prof. D. Günther for the Pt content analysis. Financial support by the Swiss Commission for Technology and Innovation (CTI grant 5978.2) and ETH (TH Project Nr. 32/03-3) is gratefully acknowledged.

CM050538+